Avoided crossings and bound states in the continuum in low-contrast dielectric gratings

Evgeny N. Bulgakov and Dmitrii N. Maksimov
Reshetnev Siberian State University of Science and Technology, 660037 Krasnoyarsk, Russia
and Kirensky Institute of Physics, Federal Research Center KSC SB RAS, 660036 Krasnoyarsk, Russia

(Received 26 July 2018; published 21 November 2018)

We consider bound states in the continuum (BICs) in low-contrast dielectric gratings. It is demonstrated that the BICs originate from the reduced guided modes on the effective dielectric slab with the permittivity equal to the average permittivity of the dielectric grating. In the case of isolated resonances, the positions of BICs can be found from two-wave dispersion relationships for guided leaky modes. In the case of the degeneracy between the two families of leaky modes, the system exhibits an avoided crossing of resonances. In the spectral vicinity of the avoided crossing the transmittance as well as the emergence of BICs is described in the framework of the generic formalism by Volya and Zelevinsky [Phys. Rev. C **67**, 054322 (2003)] with a single fitting parameter.

DOI: 10.1103/PhysRevA.98.053840

I. INTRODUCTION

Controlling the localization of electromagnetic waves through engineering high-quality resonances is of fundamental importance in electromagnetesm [1,2]. Several platforms have been investigated from microwaves to optics towards minimizing radiation losses including whispering gallery modes [3], metasurfaces [4], photonic crystal microcavities [5], dielectric resonators [6,7], and Fabry-Pérot structures [8]. Among those platforms dielectric gratings (DGs) have become an important instrument in optics with various applications relying on high-quality resonances [1,8]. In particular ultra-high-quality resonances were demonstrated in the spectral vicinity of the avoided crossings of the DG modes [9].

The utmost case of light localization in dielectric structures is the emergence of bound states in the continuum (BICs), i.e., localized eigenmodes of Maxwell's equations with the infinite quality factor embedded into the continuous spectrum of the scattering states [2]. In the recent past, the optical BICs were experimentally observed in all-dielectric setups with periodically varying permittivity [10,11]. The BICs have been extensively studied in various types of grated structures ranging from the simplest case of an array of rectangular bars in air [11,12] to substarate gratings [13] and grated fibers [14,15].

In this paper, we consider BICs in planar DGs consisting of laterally arranged rectangular bars made of two dielectric materials with a small difference in dielectric permittivity, see Fig. 1. Thus, the DG is a dielectric slab of thickness h in the z direction with stepwise alternating permittivity with period a along the x axis.

The bars with permittivity ϵ_1 have thickness b in the x direction, whereas the bars with ϵ_2 have thickness a-b. The grating is infinitely extended in both x and y directions. Since the difference in permittivity between the neighboring bars is small with respect to the absolute values we will term such a system as *low contrast* DGs to emphasize the low dielectric contrast between the building blocks of the grating. To avoid disambiguity, we stress at the outset that the dielectric contrast between the grating itself and the surrounding medium (air) can be arbitrary.

The generic mechanism of the BIC formation was put forward in 1985 by Friedrich and Wintgen, who demonstrated [16] that a BIC occurs as a product of destructive interference of two resonant modes coupled to the outgoing channel. Here we show that the low-contrast DGs support BICs at any small dielectric contrast between the bars due to interference between two nonorthogonal leaky modes [17] in the spectral vicinity of avoided crossings. The results are verified against straightforward simulations with rigorous coupled wave analysis (RCWA) [18].

Due to the system's translational symmetries the spectral parameters of the free-space eigenmodes are linked through the following dispersion relationship [19]:

$$k_0^2 = k_{x,n}^2 + k_z^2 + k_y^2, \quad k_{x,n} = \beta + 2\pi n/a, \tag{1}$$

where k_0 is the vacuum wave number, $k_{x,z}$'s are the wave numbers along the x, y axes, k_z is the far-field wave number in the direction orthogonal to the plane of the structure, β is the Bloch wave number (propagation constant), and, finally, $n = 0, \pm 1, \ldots$ corresponds to the diffraction order. Here, we consider transverse magnetic (TM) modes with $k_y = 0$, i.e., propagating only perpendicular to the bars. The analysis will be performed in the spectral range,

$$\beta a < k_0 a < 2\pi - \beta a, \tag{2}$$

which according to Eq. (1) means that only one TM scattering channel is open in the far zone on both sides of the DG.

The TM modes are the solutions of the scalar wave equation,

$$\nabla^2 \psi(x,z) + \epsilon(x,z) k_0^2 \psi(x,z) = 0, \tag{3}$$

where $\epsilon(x,z)$ is the dielectric permittivity and $\psi(x,z)$ is the y component of the electric vector $\psi(x,z) = E_y(x,z)$. Following Ref. [14] we expand the dielectric permittivity into

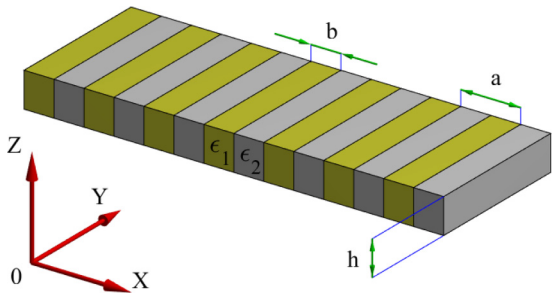

FIG. 1. Grating composed of dielectric bars with different permittivities ϵ_1 and ϵ_2.

Fourier harmonics,

$$\epsilon(x,z)=\sum_{n=-\infty}^{\infty}\gamma_n e^{i2\pi nx/a}. \tag{4}$$

In low-contrast DGs, the following condition always holds true:

$$|\gamma_0|\gg|\gamma_n|,\quad n\neq 0. \tag{5}$$

Retaining only γ_0 in Eq. (4) would lead us to a uniform dielectric slab which does not support BICs. Thus, for finding BICs, both $\gamma_{\pm1}$ should be retained in the first-order approximation. We will see in the next section, although, that in *some* cases retaining only γ_1 (or γ_{-1}) suffices for finding the BICs to a good accuracy.

II. TWO-WAVE BICs

The solution for the EM field within the DG is written

$$\psi_s=U_s(x)\frac{\cos(\varkappa z)}{\cos(\varkappa h/2)}e^{i\beta x},$$
$$\psi_a=U_a(x)\frac{\sin(\varkappa z)}{\sin(\varkappa h/2)}e^{i\beta x}, \tag{6}$$

where $\varkappa$ is the propagation constant in the z direction within the DG and subscripts s and a stand for waves symmetric (antisymmetric) with respect to the central plane of the grating. The functions $U_{s,a}(x)$ obey the equation,

$$\left[\left(\frac{\partial}{\partial x}+i\beta\right)^2+k_0^2\epsilon(x)\right]U_{s,a}(x)=\varkappa^2U_{s,a}(x). \tag{7}$$

Let us write $U_{s,a}(x)$ in the following form:

$$U_{s,a}(x)=\sum_{n=-\infty}^{\infty}u_n e^{i2\pi nx/a}. \tag{8}$$

As shown [14] under the condition that γ_0 and γ_1 are retained in Eq. (4) we have to retain u_0 and u_{-1} in Eq. (8) to derive self-consistent equations from Eq. (7). Those equations read [14]

$$\left(\gamma_0k_0^2-\beta^2\right)u_0+\gamma_1k_0^2u_{-1}=\varkappa^2u_0,$$
$$\left[\gamma_0k_0^2-\left(\beta-\frac{2\pi}{a}\right)^2\right]u_{-1}+\gamma_1k_0^2u_0=\varkappa^2u_{-1}. \tag{9}$$

The symmetric (antisymmetric) waves can be excited if the DG is symmetrically (antisymmetrically) illuminated by monochromatic plane waves from both sides. The general symmetric solution outside the grating $z>|h/2|$ reads

$$\psi(x,z)=e^{i\beta x}\left(A\frac{e^{-ik_{z,0}|z|}}{e^{-ik_{z,0}h/2}}+\sum_n t_n\frac{e^{ik_{z,n}|z|+i2\pi nx/a}}{e^{ik_{z,n}h/2}}\right), \tag{10}$$

where A is the amplitude of the incident wave,

$$k_{z,n}=\sqrt{k_0^2-\left(\beta+\frac{2\pi n}{a}\right)^2}, \tag{11}$$

and t_n's are the amplitudes of the outgoing waves. The antisymmetric solution only differs from Eq. (10) by its sign in the upper half-space. To be consistent with the two-wave approximation, the summation runs $n=0,-1$. Thus, the total solution is given by four unknown quantities u_0, u_{-1}, t_0, and t_{-1}. By using Eqs. (6) and (8)–(10) together with the interface boundary conditions [14], we find

$$\begin{pmatrix}J_0+J_{-1}\sigma_{-1}^2+(1+\sigma_{-1}^2)ik_{z,0} & \sigma_{-1}(J_{-1}-J_0)\\ \sigma_{-1}(J_{-1}-J_0) & J_{-1}+J_0\sigma_{-1}^2+(1+\sigma_{-1}^2)ik_{z,-1}\end{pmatrix}\begin{pmatrix}t_0\\ t_{-1}\end{pmatrix}=A\begin{pmatrix}ik_{z,0}(1+\sigma_{-1}^2)-J_0-J_{-1}\sigma_{-1}^2\\ -\sigma_{-1}(J_{-1}-J_0)\end{pmatrix}, \tag{12}$$

where

$$J_n=\begin{cases}\varkappa_n\tan(\varkappa_nh/2), & \text{symmetric waves},\\ -\varkappa_n\cot(\varkappa_nh/2), & \text{antisymmetric waves},\end{cases} \tag{13}$$

with

$$\sigma_{-1}=\frac{\gamma_1k_0^2}{f_{-1}^2-f_0^2}, \tag{14}$$

$$\varkappa_{-1}^2=f_{-1}^2+\frac{\gamma_1^2k_0^4}{f_{-1}^2-f_0^2}, \tag{15}$$

$$\varkappa_0^2=f_0^2-\frac{\gamma_1^2k_0^4}{f_{-1}^2-f_0^2}, \tag{16}$$

$$f_n=\sqrt{\gamma_0k_0^2-\left(\beta+\frac{2\pi n}{a}\right)^2}. \tag{17}$$

A BIC is a source-free solution decoupled from the open decay channel. Setting $A=0$, $t_0=0$ in Eq. (12) with nonzero t_{-1} leads to

$$J_0=J_{-1}, \tag{18}$$

$$-ik_{z,-1}=J_{-1}. \tag{19}$$

One the other hand, it immediately follows from Eqs. (18) and (19) that the determinant of the matrix in Eq. (12) is zero and Eq. (12) is solvable for $A = 0$. Thus, Eqs. (18) and (19) are the condition for the BICs. By close examination of Eq. (12), one finds that in the limit $\gamma_1 = 0$ Eq. (19) becomes the dispersion equation of the reduced bands folded to the Brillouin zone for a uniform slab of permittivity γ_0, which according to Eq. (4) is the average dielectric permittivity of the DG.

We see now that in the two-wave approximation the BICs originate from the reduced guided modes on a uniform dielectric slab under an extra condition Eq. (18). Essentially the same result could be obtained by considering a two mode approximation with account of γ_{-1} instead of γ_1 and u_1 instead of u_{-1}. This approximation yields the same formulas with $n = 1$ instead of $n = -1$,

$$J_0 = J_1, \tag{20}$$

$$-ik_{z,1} = J_1. \tag{21}$$

In Fig. 2(a), we demonstrate the reduced bands (folded to the Brillouin zone) of a uniform dielectric slab with the effective permittivity γ_0 in the spectral range Eq. (2). The bands are found by solving the dispersion equations (19) and (21) with $\gamma_1 = 0$. The transmittance for the low-contrast DG under illumination by a plane wave from the upper half-space computed with the use of RCWA is plotted in Fig. 2(b). By comparing Fig. 2(a) against Fig. 2(b), one can see that each reduced guided mode on the dielectric slab corresponds to an isolated high-quality resonance in the transmittance spectrum. In the framework of the RCWA, the solution is found in the following form:

$$\psi(x, z) = \sum_{n=-\infty}^{\infty} S_n(z) e^{ik_{x,n}x}. \tag{22}$$

In Figs. 3(a) and 3(b) we show the mode shape of a BIC hosted by an antisymmetric leaky mode along with the bar diagram showing the expansion coefficients $S_n(z)$ obtained by the RCWA. One can see from Fig. 3 that $S_0(z)$, $S_{-1}(z)$ dominate in the expansion. In the inset to Fig. 3(a) we demonstrate the dispersion of the Q factor for the leaky mode hosting the BIC found with both the RCWA and the two-wave approximation Eq. (12). Again, similar to Ref. [14], the two-wave mode predicts the behavior of the Q factor to good accuracy.

Finally, let us briefly discuss the accuracy of the approximation introduced in this section. It is seen from Fig. 3(a) that, other than u_{-1}, u_0 expansion coefficients, noticeably u_{-2}'s are present in the RCWA solution. One can estimate u_{-2} by applying the Rayleigh-Schrödinger perturbation theory [20] to the zeroth-order solution with the only nonzero term u_{-1}. The result reads

$$u_{-2} = \frac{\gamma_1 k_0^2}{f_{-2}^2 - f_{-1}^2} u_{-1}, \tag{23}$$

whereas the same approach for u_0 yields

$$u_0 = \frac{\gamma_1 k_0^2}{f_{-1}^2 - f_0^2} u_{-1}. \tag{24}$$

The above equations predict $|u_{-2}/u_0| \approx 0.2$ and $|u_{-2}/u_{-1}| \approx 10^{-2}$ for the BIC shown in Fig. 3(b). That is in qualitative agreement with the data plotted in Fig. 3(a). Numerically, the deviations are reflected in a small difference between the position of the BIC found from the RCWA ($ak_0 = 4.0565$, $a\beta = 1.3715$) and the two-wave approximation Eqs. (18) and (19) ($ak_0 = 4.0576$, $a\beta = 1.3708$).

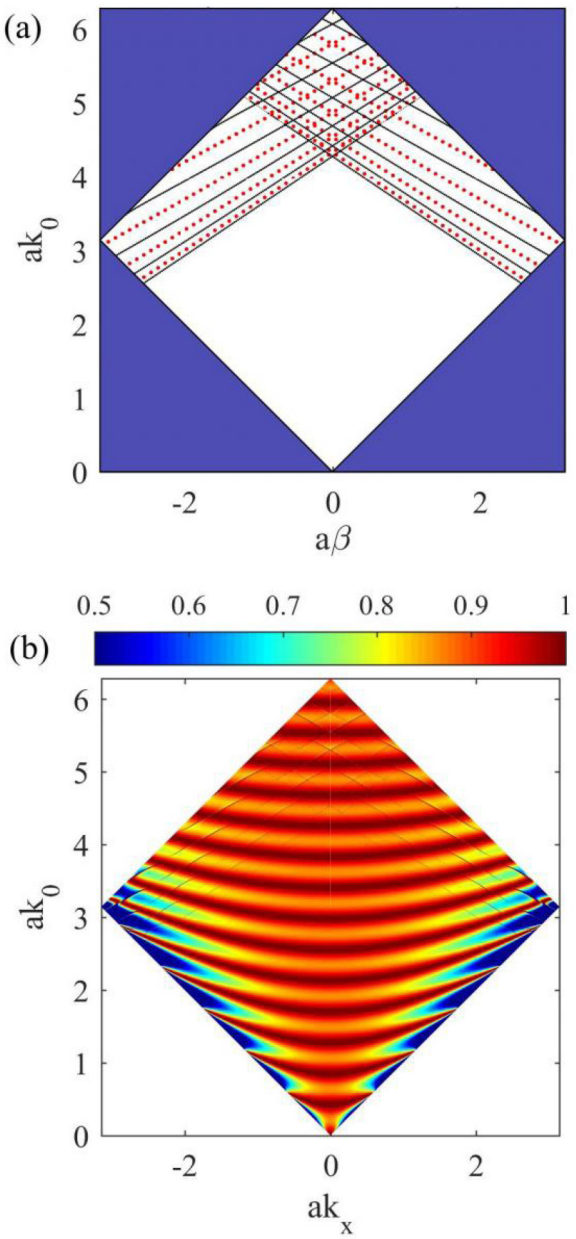

FIG. 2. Transmittance spectra of a low-contrast DG, $h = 5a$, $b = a/2$, $\epsilon_1 = 2.0736$, $\epsilon_2 = 2.2801$ (fused silica and soda lime glass at 1.861 μm, respectively). (a) Reduced bands on a dielectric slab with effective permittivity γ_0, solid black lines: symmetric modes; red dots: antisymmetric modes. (b) Transmittance spectrum of the DG under illumination by a monochromatic plane wave from the upper half-space obtained by RCWA.

III. THREE-WAVE BICs

The two-wave approximation breaks down in the spectral vicinity of the crossing between the guided modes in Fig. 2(a). In those points all three leading coefficients γ_{-1}, γ_0, and γ_1

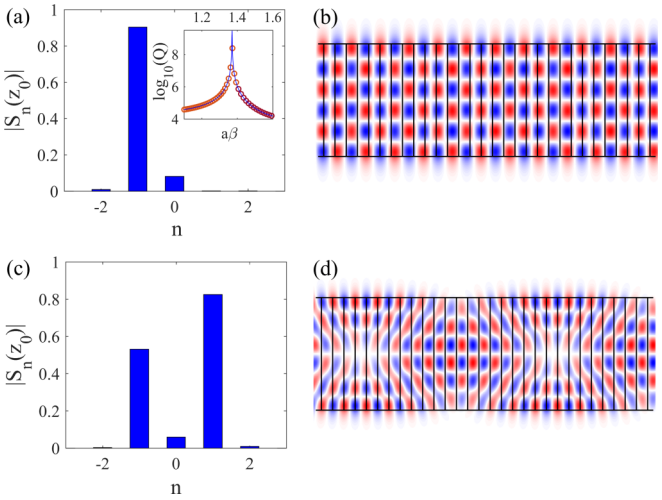

FIG. 3. BICs in low-contrast DGs; two-wave BIC found with RCWA $ak_0 = 4.0565$, $a\beta = 1.3715$, (a) bar diagram for $S_n(z_0)$, $z_0 = h/6$; the inset shows the dispersion of the Q factor in the spectral vicinity of the BIC, solid blue: two-wave approximation; red circles: RCWA, (b) the BIC mode shape Re$\{\psi\}$; three-wave BIC found with RCWA $ak_0 = 5.0941$, $a\beta = 0.36712$, (c) bar diagram for $S_n(z_0)$, $z_0 = h/6$, (d) the BIC mode shape Re$\{\psi\}$. The optogeometric parameters are the same as in Fig. 2.

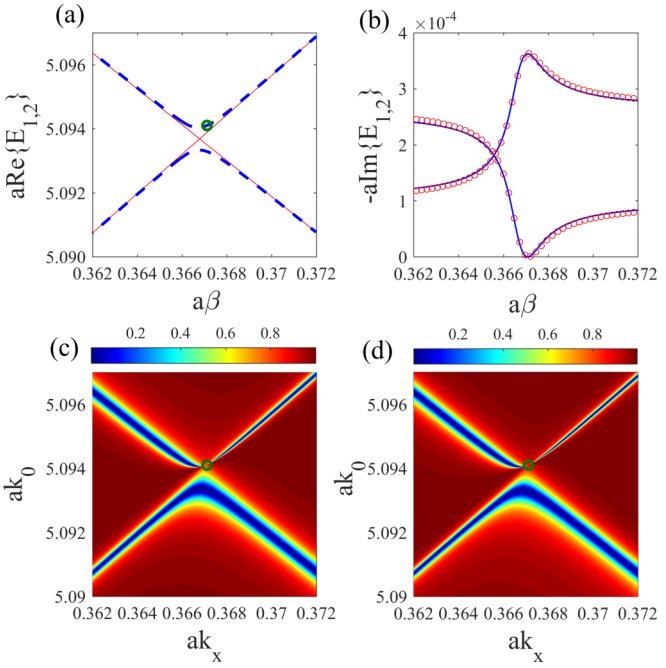

FIG. 4. BIC in the spectral vicinity of an avoided crossing. (a) The real part of the eigenvalues of $\widehat{\mathcal{H}}$ with $v = 3.5\times10^{-4}$—dashed blue lines and the positions of the unperturbed resonances—solid red. (b) The imaginary part of the eigenvalues of $\widehat{\mathcal{H}}$ with $v = 3.5\times10^{-4}$ (solid blue line) and RCWA data (red circles). (c) The transmittance found from Eq. (26). (d) The transmittance found with RCWA. The position of the BIC is shown by a green circle. The optogeometric parameters are the same as in Fig. 2.

must be taken into account. It is technically possible to find an analytical solution in such a three-wave approximation. This, however, results in awkward expressions for the eigenvalues of the 3×3 matrix. The analytical results are collected in the Appendix. In this section, we spare the reader of the cumbersome mathematics applying a generic scattering theory for two spectrally close nonorthogonal resonances proposed by Volya and Zelevinsky [17]. We mention in passing that the above approach is generic for two-mode settings [21]. For justification of applying the formalism by Volya and Zelevinsky [17] we again address the reader to the Appendix.

The interference of two nonorthogonal resonances is described by the effective non-Hermitian operator,

$$\widehat{\mathcal{H}} = \begin{Bmatrix} \omega_1 & v \\ v & \omega_{-1} \end{Bmatrix} - i \begin{Bmatrix} \Gamma_{-1} & \sqrt{\Gamma_1\Gamma_{-1}} \\ \sqrt{\Gamma_1\Gamma_{-1}} & \Gamma_{-1} \end{Bmatrix}, \qquad (25)$$

where $\omega_{1,-1}$'s are the real parts of the complex eigenfrequency of the unperturbed resonant leaky mode, $\Gamma_{1,-1}$'s are the corresponding resonant widths, and v reflects the nonorthogonality between the leaky modes. Note that in the above equation we use the indices $1, -1$ rather than 1,2 to underline the link with the expression presented in the Appendix. In the above definition the transmission amplitude is given by [21]

$$t_0 = 2\frac{\omega(\Gamma_1 + \Gamma_{-1}) - \Gamma_1\omega_{-1} - \Gamma_{-1}\omega_1 + v\sqrt{\Gamma_1\Gamma_{-1}}}{(\omega - E_1)(\omega - E_2)}, \qquad (26)$$

where $E_{1,2}$'s are the eigenvalues of $\widehat{\mathcal{H}}$ whereas the condition for a BIC has the following form:

$$v(\Gamma_1 - \Gamma_{-1}) = \sqrt{\Gamma_1\Gamma_{-1}}(\omega_1 - \omega_{-1}). \qquad (27)$$

The positions of the unperturbed resonances $\omega_{1,-1}$ can be found from the transmittance spectra obtained by the RCWA away from the point of the avoided crossing. Then, $\Gamma_{1,-1}$ can be found by solving Eq. (12) in the two-wave approximation outlined in the previous section or explicitly from Eq. (A20). Thus, we are left with the only unknown fitting parameter v. In Figs. 4(a) and 4(b), we show the real and imaginary parts of the eigenvalues of $\widehat{\mathcal{H}}$ obtained by fitting Eq. (26) to the exact transmittance spectrum obtained by the RCWA in the vicinity of an avoided crossing. The positions of the unperturbed resonances are also shown in Fig. 4(a). The imaginary parts of the resonant eigenvalues obtained by the RCWA are shown in Fig. 4(b). Finally, in Figs. 4(c) and 4(d) we compare Eq. (26) against an exact numerical transmittance spectrum. One can see from Figs. 4(c) and 4(d) that the results coincide to good accuracy. The position of a BIC given by Eq. (27) also coincides with the numerical data. In Figs. 3(c) and 3(d), we show the mode shape of the free-wave BIC along with the bar diagram for $S_n(z)$. One can see that now three waves $n = -1, 0, 1$ dominate in the expansion.

IV. CONCLUSION

To summarize, we recovered the generic mechanism for BICs in low-contrast DGs. It is shown that the BICs originate from the reduced guided modes on the effective dielectric slab with the permittivity equal to the average permittivity of the DG. In the case of isolated resonances the positions of BICs can be found from two-wave dispersion relationships for guided leaky modes as is previously demonstrated for fiber gratings [14]. In the case of the degeneracy between the two families of leaky modes, the system exhibits an avoided

crossing of resonances. We demonstrated that the occurrence of the avoided crossing can be quantitatively explained by a perturbative solution of the tree-wave model. Numerically, in the spectral vicinity of the avoided crossing the transmittance as well as the emergence of BICs is well described in the framework of the generic formalism by Volya and Zelevinsky [17] with a single fitting parameter. We speculate that ultra-high-quality resonances previously reported in the literature [9] can be attributed to the emergence of BICs. Notice that Eq. (26) is always fulfilled in the Γ point. Thus, the only condition for BIC is the presence of leaky modes in the spectral range Eq. (2). If the guided modes are supported on the slab with the average permittivity γ_0, BICs always exist no matter how small the dielectric contrast is. Recently, we have seen some interest in light localization and transmittance Fano line shapes due to interference of two resonances [7,22]. So far the link between avoided crossings and BICs has been mostly investigated in quantum systems [17,21,23] and was only recently underlined in the realm of optics [24]. We believe that the results presented may be helpful in engineering BICs in optical setups, such as DGs.

ACKNOWLEDGMENTS

This work was supported by Ministry of Education and Science of the Russian Federation (State Contract No. 3.1845.2017/4.6). We are grateful to K. N. Pichugin for assistance with the computations.

APPENDIX: ANALYTICAL APPROACH TO THREE-WAVE BICs

Let us consider analytical solution of Eq. (7) when three Fourier components are taken into account in Eq. (8),

$$U_{s,a}(x) = u_1 e^{i2\pi x/a} + u_0 + u_{-1} e^{-i2\pi x/a}. \tag{A1}$$

In full analog with Eq. (9) we have

$$\begin{aligned} f_0^2 u_0 + \gamma_1 k_0^2 (u_{-1} + u_1) &= \varkappa^2 u_0, \\ \gamma_1 k_0^2 u_0 + f_1^2 u_1 &= \varkappa^2 u_1, \\ \gamma_1 k_0^2 u_0 + f_{-1}^2 u_{-1} &= \varkappa^2 u_{-1}, \end{aligned} \tag{A2}$$

where f_n is given by Eq. (17). Note that the terms with γ_2 are absent Eq. (9) since $\gamma_2 = 0$ for $b = a/2$ as defined in Fig. 1. In the above equation we face an eigenvalue problem for the 3×3 matrix. Although such a problem could be solved analytically with the use of Cardano's method that would result in cumbersome expressions rendering the result unsuitable for further analysis. Here we restrict ourselves with a perturbative analysis up to the terms $O(\gamma_1^3)$. Then, the tree solutions Eq. (A2) of the eigenvalue problem read

$$\begin{aligned} \varkappa_{-1}^2 &= f_{-1}^2 + \frac{\gamma_1^2 k_0^4}{f_{-1}^2 - f_0^2}, \\ \varkappa_1^2 &= f_1^2 + \frac{\gamma_1^2 k_0^4}{f_1^2 - f_0^2}, \\ \varkappa_0^2 &= f_0^2 - \frac{\gamma_1^2 k_0^4}{f_{-1}^2 - f_0^2} - \frac{\gamma_1^2 k_0^4}{f_1^2 - f_0^2}. \end{aligned} \tag{A3}$$

The corresponding eigenvectors $\mathbf{u}_n = (u_{-1}, u_0, u_1)$ read

$$\mathbf{u}_{-1} = \begin{pmatrix} 1 \\ \sigma_{-1} \\ 0 \end{pmatrix}, \quad \mathbf{u}_1 = \begin{pmatrix} 0 \\ \sigma_1 \\ 1 \end{pmatrix}, \quad \mathbf{u}_0 = \begin{pmatrix} \sigma_{-1} \\ -1 \\ \sigma_1 \end{pmatrix}, \tag{A4}$$

where

$$\sigma_n = \frac{\gamma_1 k_0^2}{f_n^2 - f_0^2}. \tag{A5}$$

Importantly, unlike Eq. (A4), in Eq. (A4) we only retained the terms up to $O(\gamma_1^2)$. This is because the second-order Rayleigh-Schrödinger perturbation approach for eigenvectors results in bulky expressions [20] which enormously complicate further analysis. Returning to Eq. (6) one can write the general solution inside the slab as

$$\begin{aligned} \psi(x,z) = e^{i\beta x} [& C_{-1}(\sigma_{-1} + e^{-i2\pi x/a}) F_{-1}(z) \\ & + C_1(\sigma_1 + e^{i2\pi x/a}) F_1(z) \\ & + C_0(1 - \sigma_{-1} e^{-i2\pi x/a} - \sigma_1 e^{i2\pi x/a}) F_0(z)], \end{aligned} \tag{A6}$$

where C_{-1}, C_0, and C_1 are unknown coefficients to be defined from matching with the solution outside the grating Eq. (10) and the functions $F_n(z)$ are given by

$$F_n(z) = \begin{cases} \frac{\cos(\varkappa_n z)}{\cos(\varkappa_n h/2)}, & \text{symmetric waves,} \\ \frac{\sin(\varkappa_n z)}{\sin(\varkappa_n h/2)}, & \text{antisymmetric waves.} \end{cases} \tag{A7}$$

By applying the interface boundary conditions one can remove the unknowns C_{-1}, C_0, and C_1 ending up with a set of equations for the amplitudes of the outgoing waves t_{-1}, t_0, and t_1,

$$\begin{pmatrix} -J_0 - J_{-1}\sigma_{-1}^2 - J_1\sigma_1^2 & (J_0 - J_{-1})\sigma_{-1} & (J_0 - J_1)\sigma_1 \\ (J_0 - J_{-1})\sigma_{-1} & -J_0\sigma_{-1}^2 - J_{-1}(1+\sigma_1^2) & (J_{-1} - J_0)\sigma_{-1}\sigma_1 \\ (J_0 - J_1)\sigma_1 & (J_1 - J_0)\sigma_{-1}\sigma_1 & -J_0\sigma_1^2 - J_1(1+\sigma_{-1}^2) \end{pmatrix} \begin{pmatrix} t_0 + A \\ t_{-1} \\ t_1 \end{pmatrix} = i\left(1 + \sigma_{-1}^2 + \sigma_1^2\right) \begin{pmatrix} k_{z,0}(t_0 - A) \\ k_{z,-1} t_{-1} \\ k_{z,1} t_1 \end{pmatrix}, \tag{A8}$$

where we again omitted all terms $O(\gamma_1^3)$. The solution of Eq. (A8) can be written in the following form:

$$t_0 = -A - \frac{2ik_{z,0}DA(\tilde{\Sigma}_1 + \tilde{\Sigma}_{-1} + D\tilde{\Sigma}_1\tilde{\Sigma}_{-1})}{Z_0}, \tag{A9}$$

$$t_{-1} = -\frac{2ik_{z,0}DA}{\sigma_{-1}Z_{-1}}, \tag{A10}$$

$$t_1 = -\frac{2ik_{z,0}DA}{\sigma_1 Z_1}, \tag{A11}$$

$$Z_0 = \tilde{E}_1(J_0 - J_{-1} - \tilde{\Sigma}_0) + \tilde{\Sigma}_{-1}(J_0 - J_1 - \tilde{\Sigma}_0) - D\tilde{\Sigma}_0\tilde{\Sigma}_1\tilde{\Sigma}_{-1}, \tag{A12}$$

$$Z_{-1} = J_0 - J_{-1} - \tilde{\Sigma}_0(1 + \tilde{\Sigma}_{-1}D) + \frac{\tilde{\Sigma}_{-1}}{\tilde{\Sigma}_1}(J_0 - J_1 - \tilde{\Sigma}_0), \tag{A13}$$

$$Z_1 = J_0 - J_1 - \tilde{\Sigma}_0(1 + \tilde{\Sigma}_1 D) + \frac{\tilde{\Sigma}_1}{\tilde{\Sigma}_{-1}}(J_0 - J_{-1} - \tilde{\Sigma}_0) \tag{A14}$$

$$\tilde{\Sigma}_0 = J_0 + ik_{0,z} + J_{-1}\sigma_{-1}^2 + J_1\sigma_1^2 + ik_{0,z}\left(\sigma_1^2 + \sigma_{-1}^2\right), \tag{A15}$$

and

$$D = 1 + \sigma_{-1}^2 + \sigma_1^2 \tag{A16}$$

$$\tilde{\Sigma}_{-1} = \frac{\tilde{\epsilon}_{-1}}{\sigma_{-1}^2(J_0 - J_{-1})}, \tag{A17}$$

$$\tilde{\Sigma}_1 = \frac{\tilde{\epsilon}_1}{\sigma_1^2(J_0 - J_1)}, \tag{A18}$$

$$\tilde{\epsilon}_n = ik_{z,n} + J_n. \tag{A19}$$

Note that, after setting $\sigma_1 = 0$, Eq. (A8) formally coincides with Eq. (12). On more rigorous grounds the two-wave approximation can be justified by considering the quantities $\tilde{\Sigma}_{-1}, \tilde{\Sigma}_1$, which are generally diverging since σ_{-1}, σ_1 are vanishing with γ_1 according to Eq. (A5). This, however, is not the case if $\tilde{\epsilon}_{-1} \to 0$. In that situation, according to Eqs. (A13) and (A14) we have $|Z_{-1}| \gg |Z_1|$ and, consequently, $|t_{-1}| \gg |t_1|$ as one can see from Eqs. (A10) and (A11). The latter inequality allows us to drop t_1 from Eq. (A8). Remarkably, the aforementioned condition $\tilde{\epsilon}_{-1} \to 0$ is equivalent to Eq. (19) as is easily seen from Eq. (A19). The same arguments equally apply for the two-wave approximation with only u_0, u_1 taken into account when $\tilde{\epsilon}_1 \to 0$. By extracting the imaginary parts of the denominator in Eqs. (A11) and (A10), one can find the resonant widths in the spectral vicinity of the two-wave BICs in the following form:

$$\Gamma_n = \left.\frac{\sigma_n^2(J_0 - J_n)^2 k_{z,0}}{|\tilde{\Sigma}_0|^2 \tilde{\epsilon}_n'}\right|_{k_0=\omega_0}, \tag{A20}$$

where $\tilde{\epsilon}_n'$ is the derivative of $\tilde{\epsilon}_n$ with respect to k_0 and ω_0 is the resonant eigenfrequency.

In the spectral vicinity of a BIC the resonant properties of the DG are characterized as the positions of the poles of the reflection coefficient t_0, Eq. (A9). The position of the poles E_j correspond to the complex eigenvalues of Maxwell's equations with real parts $\mathrm{Re}\{E_j\}$ corresponding to the resonant frequency whereas $-\mathrm{Im}\{E_j\}$'s are the width of the resonances. The poles can be found from analytic continuation of Eq. (A12) to the complex plane. In the case of isolated resonances associated with two-wave BICs, the analysis can be, however, simplified by allying Eq. (A20). In Fig. 5, we plot the imaginary part of the resonant eigenvalue in the spectral vicinity of the BICs from Fig. 3(a) in comparison with the resonant width found from RCWA simulations. One can note from Fig. 5 that Eq. (A20) allows for finding Γ to a good accuracy since the position of the resonance ω_0 is known from the dispersion equations (19) and (21) in the limit $\gamma_1 \to 0$.

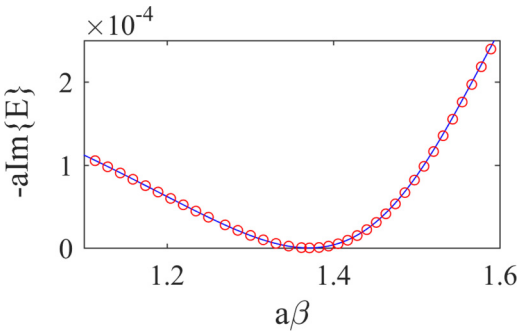

FIG. 5. The imaginary part of the resonant eigenfrequency for the leaky mode hosting the BIC from Fig. 3(a), solid blue: RCWA data; red circles: Eq. (A20).

The situation complicates, although, when both $\tilde{\Sigma}_{-1}, \tilde{\Sigma}_1$ become vanishing. By recollecting that Eqs. (19) and (21)

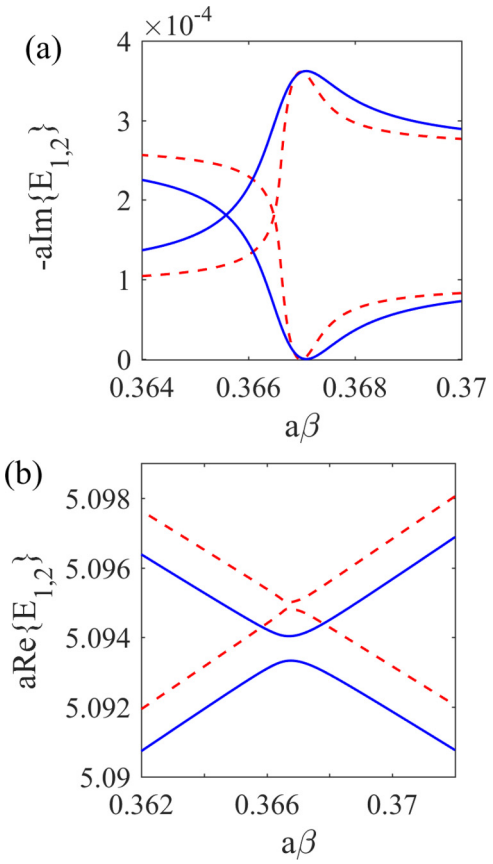

FIG. 6. Resonant eigenvalues in the spectral vicinity of an avoided crossing. (a) The imaginary parts of the resonant eigenvalues in the vicinity of the avoided crossing, solid blue: RCWA; dashed red lines: analytic continuation of Eq. (A12). (b) The real parts of the resonant eigenvalues in the vicinity of the avoided crossing, solid blue: RCWA; dashed red lines: analytic continuation of Eq. (A12).

with $\gamma_1 \to 0$ are the dispersion equations for the uniform dielectric slab, we immediately see that $\tilde{\epsilon}_n$, Eq. (A19), is small for $n = \pm 1$ at the intersection of the guided modes on the uniform dielectric slab. Then, according to Eqs. (A17) and (A18), both $\tilde{\Sigma}_{-1}$, $\tilde{\Sigma}_1$ are vanishing. In Fig. 6, we compare the the resonant eigenvalues extracted from RCWA simulations against the position of the poles of the transmission coefficients, Eq. (A9). In both cases, we found two eigenvalues $E_{1,2}$ with vanishing Γ. In Fig. 6(a), we show the imaginary parts. One can see that the two approaches are in qualitative agreement with one another, both predicting a vanishing resonant width. The real parts of $E_{1,2}$ also demonstrate a qualitative agreement between the two approaches as seen from Fig. 6(b). In fact, here we see an avoided crossing between the position of the poles typically for two leaky mode interference mechanisms of the BICs proposed by Volya and Zelevinsky [17].

Finally, a short remark is due on the accuracy of Eq. (A9). By comparing Eq. (A9) against Eq. (26) we find the following expression for parameter v:

$$v = \frac{J_1 + J_{-1}}{2k_{0,z}} + \frac{k_0}{J_0}. \tag{A21}$$

Numerically, Eq. (A21) underestimates v by approximately 3.5 times in comparison with the exact spectrum. We speculate that the deviations are due to $O(\gamma_1^2)$ terms dropped from Eq. (A4). Nonetheless, the three-wave model analyzed here is capable of both predicting the spectra of all isolated resonances to a good accuracy (see Fig. 5) and qualitatively describing their avoided crossing (see Fig. 6).

[1] S. John, Nat. Mater. **11**, 997 (2012); D. Marpaung, C. Roeloffzen, R. Heideman, A. Leinse, S. Sales, and J. Capmany, Laser Photon. Rev. **7**, 506 (2013); P. Qiao, W. Yang, and C. J. Chang-Hasnain, Adv. Opt. Photon. **10**, 180 (2018).

[2] C. W. Hsu, B. Zhen, A. D. Stone, J. D. Joannopoulos, and M. Soljačić, Nat. Rev. Mater. **1**, 16048 (2016).

[3] M. L. Gorodetsky and V. S. Ilchenko, J. Opt. Soc. Am. B **16**, 147 (1999); J. Zhu, S. K. Ozdemir, Y.-F. Xiao, L. Li, L. He, D.-R. Chen, and L. Yang, Nat. Photon. **4**, 46 (2009).

[4] I. A. I. Al-Naib, C. Jansen, and M. Koch, Appl. Phys. Lett. **94**, 153505 (2009); C. Jansen, I. A. I. Al-Naib, N. Born, and M. Koch, *ibid.* **98**, 051109 (2011); R. Singh, W. Cao, I. Al-Naib, L. Cong, W. Withayachumnankul, and W. Zhang, *ibid.* **105**, 171101 (2014); A. Krasnok and A. Alú, J. Opt. **20**, 064002 (2018).

[5] T. Tanabe, M. Notomi, E. Kuramochi, A. Shinya, and H. Taniyama, Nat. Photon. **1**, 49 (2007); S. Noda, M. Fujita, and T. Asano, *ibid.* **1**, 449 (2007).

[6] T. Lepetit, E. Akmansoy, J.-P. Ganne, and J.-M. Lourtioz, Phys. Rev. B **82**, 195307 (2010); T. Lepetit and B. Kanté, *ibid.* **90**, 241103(R) (2014).

[7] M. V. Rybin, K. L. Koshelev, Z. F. Sadrieva, K. B. Samusev, A. A. Bogdanov, M. F. Limonov, and Y. S. Kivshar, Phys. Rev. Lett. **119**, 243901 (2017).

[8] P. Velha, E. Picard, T. Charvolin, E. Hadji, J. Rodier, P. Lalanne, and D. Peyrade, Opt. Express **15**, 16090 (2007); A. R. M. Zain, N. P. Johnson, M. Sorel, and R. M. D. L. Rue, *ibid.* **16**, 12084 (2008); C. J. Chang-Hasnain and W. Yang, Adv. Opt. Photon. **4**, 379 (2012).

[9] V. Karagodsky, C. Chase, and C. J. Chang-Hasnain, Opt. Lett. **36**, 1704 (2011).

[10] Y. Plotnik, O. Peleg, F. Dreisow, M. Heinrich, S. Nolte, A. Szameit, and M. Segev, Phys. Rev. Lett. **107**, 183901 (2011); S. Weimann, Y. Xu, R. Keil, A. E. Miroshnichenko, A. Tünnermann, S. Nolte, A. A. Sukhorukov, A. Szameit, and Y. S. Kivshar, *ibid.* **111**, 240403 (2013); C. W. Hsu, B. Zhen, J. Lee, S.-L. Chua, S. G. Johnson, J. D. Joannopoulos, and M. Soljačić, Nature (London) **499**, 188 (2013); R. A. Vicencio, C. Cantillano, L. Morales-Inostroza, B. Real, C. Mejía-Cortés, S. Weimann, A. Szameit, and M. I. Molina, Phys. Rev. Lett. **114**, 245503 (2015); Z. F. Sadrieva, I. S. Sinev, K. L. Koshelev, A. Samusev, I. V. Iorsh, O. Takayama, R. Malureanu, A. A. Bogdanov, and A. V. Lavrinenko, ACS Photon. **4**, 723 (2017); Y.-X. Xiao, G. Ma, Z.-Q. Zhang, and C. T. Chan, Phys. Rev. Lett. **118**, 166803 (2017).

[11] J. M. Foley, S. M. Young, and J. D. Phillips, Phys. Rev. B **89**, 165111 (2014).

[12] B. Zhen, C. W. Hsu, L. Lu, A. D. Stone, and M. Soljačić, Phys. Rev. Lett. **113**, 257401 (2014); C. Blanchard, J.-P. Hugonin, and C. Sauvan, Phys. Rev. B **94**, 155303 (2016); Z. Wang, H. Zhang, L. Ni, W. Hu, and C. Peng, IEEE J. Quantum Electron. **52**, 1 (2016); L. Ni, Z. Wang, C. Peng, and Z. Li, Phys. Rev. B **94**, 245148 (2016); A. Taghizadeh and I.-S. Chung, Appl. Phys. Lett. **111**, 031114 (2017).

[13] J. W. Yoon, S. H. Song, and R. Magnusson, Sci. Rep. **5**, 18301 (2015); X. Cui, H. Tian, Y. Du, G. Shi, and Z. Zhou, *ibid.* **6**, 36066 (2016); F. Monticone and A. Alù, New J. Phys. **19**, 093011 (2017); Y. Wang, J. Song, L. Dong, and M. Lu, J. Opt. Soc. Am. B **33**, 2472 (2016); E. N. Bulgakov, D. N. Maksimov, P. N. Semina, and S. A. Skorobogatov, *ibid.* **35**, 1218 (2018).

[14] X. Gao, B. Zhen, M. Soljačić, and H. Chen, C. W. Hsu, arXiv:1707.01247.

[15] E. N. Bulgakov and A. F. Sadreev, Phys. Rev. A **96**, 013841 (2017).

[16] H. Friedrich and D. Wintgen, Phys. Rev. A **32**, 3231 (1985).

[17] A. Volya and V. Zelevinsky, Phys. Rev. C **67**, 054322 (2003).

[18] M. G. Moharam and T. K. Gaylord, J. Opt. Soc. Am. **71**, 811 (1981); S. G. Tikhodeev, A. L. Yablonskii, E. A. Muljarov, N. A. Gippius, and T. Ishihara, Phys. Rev. B **66**, 045102 (2002).

[19] E. Popov, *Gratings: Theory and Numeric Applications* (Popov, Institut Fresnel, 2012).

[20] L. D. Landau and E. M. Lifshitz, *Quantum Mechanics: Non-Relativistic Theory* (Pergamon Press, London, 1958) .

[21] A. F. Sadreev, E. N. Bulgakov, and I. Rotter, Phys. Rev. B **73**, 235342 (2006).

[22] D. A. Bykov and L. L. Doskolovich, Phys. Rev. A **92**, 013845 (2015); A. A Bogdanov, K. L. Koshelev, P. V. Kapitanova, M. V. Rybin, S. A. Gladyshev, Z. F. Sadrieva, K. B. Samusev, Y. S. Kivshar, and M. F. Limonov, arXiv:1805.09265.

[23] A. Pilipchuk and A. Sadreev, Phys. Lett. A **381**, 720 (2017).

[24] S. I. Azzam, V. M. Shalaev, A. Boltasseva, and A. V. Kildishev, arXiv:1808.08244.